In vivo behavior of radioiodinated rabbit antithrombin III. Demonstration of a noncirculating vascular compartment.

T H Carlson, … , A C Atencio, T L Simon

J Clin Invest. 1984;74(1):191-199. https://doi.org/10.1172/JCI111401.

Research Article

Rabbit antithrombin III (AT), purified by heparin-agarose, was labeled with iodine-131 by either the glucose oxidase-lactoperoxidase or iodine monochloride techniques. When intravenously injected, the disappearance of the 131I-AT from plasma was characterized by rapid initial decreases, and three-exponential equations were required for best fit of the plasma disappearance curves. This rapid 131I-AT removal was not caused by denaturation, as shown by comparison with results obtained when 131I-AT was biologically screened (injected into a first rabbit, and then transferred 16 h later in whole plasma to a second for kinetic evaluation) before injection. Thus, the same rapid initial loss of plasma 131I-AT was observed with screened preparations, and the plasma fractional catabolic rates of 0.716 +/- 0.048 and 0.673 +/- 0.051 day-1 for unscreened and screened 131I-AT were not significantly different. These results support the hypothesis that a vascular-endothelial AT compartment is present in rabbit. The fractions of the total-body AT in the plasma, the vascular-endothelial and the extravascular compartments were 0.337 +/- 0.031, 0.178 +/- 0.056, and 0.485 +/- 0.069, respectively. Two three-compartment kinetic models are discussed. The first pictures AT as distributing independently between plasma and two other compartments, and the second sees AT as first passing to the vascular-endothelial compartment, and then directly into the extravascular compartment. The plasma 131I-AT kinetic data was consistent with both models, but […]

In Vivo Behavior of Radioiodinated Rabbit Antithrombin III

Demonstration of a Noncirculating Vascular Compartment

Timothy H. Carlson, A. C. Atencio, and Toby L. Simon
Departments of Biochemistry and Pathology, University of New Mexico School of Medicine, Albuquerque, New Mexico 87131

Abstract. Rabbit antithrombin III (AT), purified by heparin–agarose, was labeled with iodine-131 by either the glucose oxidase-lactoperoxidase or iodine monochloride techniques. When intravenously injected, the disappearance of the ^{131}I-AT from plasma was characterized by rapid initial decreases, and three-exponential equations were required for best fit of the plasma disappearance curves. This rapid ^{131}I-AT removal was not caused by denaturation, as shown by comparison with results obtained when ^{131}I-AT was biologically screened (injected into a first rabbit, and then transferred 16 h later in whole plasma to a second for kinetic evaluation) before injection. Thus, the same rapid initial loss of plasma ^{131}I-AT was observed with screened preparations, and the plasma fractional catabolic rates of 0.716±0.048 and 0.673±0.051 day^{-1} for unscreened and screened ^{131}I-AT were not significantly different. These results support the hypothesis that a vascular-endothelial AT compartment is present in rabbit. The fractions of the total-body AT in the plasma, the vascular-endothelial and the extravascular compartments were 0.337±0.031, 0.178±0.056, and 0.485±0.069, respectively.

Two three-compartment kinetic models are discussed. The first pictures AT as distributing independently between plasma and two other compartments, and the second sees AT as first passing to the vascular-endothelial compartment, and then directly into the extravascular compartment. The plasma ^{131}I-AT kinetic data was consistent with both models, but the sizes of the vascular-endothelial compartments were best predicted by the second. If AT catabolism was assigned to the plasma, both models generally underpredicted the whole-body radioactivities, while assignment of breakdown to the extravascular compartment generally resulted in overpredictions. This suggests that AT catabolism occurs from both plasma and extravascular compartments.

Introduction

Antithrombin III (AT)[1] has been shown to inactivate thrombin (1), Factor X_a (2), Factor IX_a (3), and the other coagulation enzymes in vitro. The high incidence of venous thrombosis among individuals with a hereditary deficiency in AT (4), and the finding of increased levels of AT-protease complexes in the circulation of individuals with disseminated intravascular-coagulation (5) demonstrate that AT is an important inhibitor of coagulation enzymes in vivo.

The in vitro rates of the AT-protease reactions are greatly enhanced by the presence of heparin (6). Enhancement of the AT-thrombin reaction rate also occurs in vivo (7), and apparently in the absence of circulating heparin (8). This effect may be mediated by a heparinlike AT cofactor that has been found on the surface of endothelial cells (9). If this AT cofactor is present on the endothelium in vivo, it would be expected to bind some of the plasma AT with which it is in contact because of its heparinlike character.

An abstract of a portion of this research was presented at the IXth International Congress on Thrombosis and Haemostasis in Stockholm, Sweden, July 5, 1983. Some of this work is taken from the dissertation of Dr. Carlson, which was submitted in partial fulfillment of Ph.D. requirements at the University of New Mexico School of Medicine.

Received for publication 22 November 1983 and in revised form 29 February 1984.

J. Clin. Invest.

0021-9738/84/07/0191/09 $1.00
Volume 74, July 1984, 191–199

1. *Abbreviations used in this paper:* ACR, absolute antithrombin III catabolic rate; AT, antithrombin III; $\bar{A}_p$, $\bar{A}_w$, and $\bar{A}_e$, antithrombin III masses in plasma, noncirculating vascular, and extravascular compartments, respectively; j_3, $j_{3\cdot5}$, and j_T, fractions of plasma, plasma plus noncirculating vascular, and total-body AT catabolized per day; A_p, A_w, and A_e, fractions of total-body antithrombin III in plasma, noncirculating vascular, and extravascular compartments, respectively; HCT, hematocrit; $^*A_p$, $^*A_w$, $^*A_e$, and $^*A_{wb}$, ^{131}I-AT in plasma, noncirculating vascular, extravascular, and whole-body compartments; $^*A_z$, ^{131}I-AT as low molecular weight catabolic products, respectively; TCB, Tris-citrate buffer.

In this investigation we studied the distribution and catabolism on AT in the intact rabbit using ^{131}I-AT. Applying in vivo kinetic methods developed to characterize the behavior of other plasma proteins (10, 11, 12, 13), we attempted to distinguish AT free in the circulation from that bound to the endothelium. Mathematical analysis of ^{131}I-AT kinetic data permitted calculation of the fractional AT distribution, as well as its catabolic rates. These results establish the rabbit as a model for study of AT in vivo.

Methods

Materials. Tosyl-glycyl-prolyl-argine-*p*-nitroanilide acetate (Chromozym TH) was obtained from Boehringer Mannheim Biochemicals, Indianapolis, IN. Thrombin, as a crude bovine preparation, was obtained from Parke, Davis and Co., Detroit, MI. Electrophoretic-grade acrylamide, *N,N'*-methylene-*bis*acrylamide, *N,N,N',N'*,-tetramethylenediamine, ammonium persulfate, sodium dodecylsulfate, 2-mercaptoethanol, Coomassie brilliant Blue R and Enzymobead (lactoperoxidase-glucose oxidase enzyme system immobilized on polyacrylamide beads) were from Bio-Rad Laboratories, Richmond, CA. Sepharose 4B was a product of Pharmacia Fine Chemicals, Div. of Pharmacia, Inc., Piscataway, NJ. Heparin (stage 14) for heparin-agarose preparation was obtained from Inolex Corp., Chicago, IL. Heparin for heparin-cofactor assay was 5,000 U/ml from Organon, Inc., West Orange, NJ. Polybrene was from Aldrich Chemical Co., Inc., Milwaukee, WI. Tris-(hydroxymethyl)-aminomethane, was a product of Sigma Chemical Co., St. Louis, MO. Iodine-125 and iodine-131 were from ICN Chemical and Radioisotopes Div., Irvine, CA, or Amersham Corp., Arlington Heights, IL. All other chemicals were reagent grade or better. Heparin-agarose was prepared as described earlier, and contained 650 μg heparin per milliliter gel (14).

Protein preparations. Rabbit AT was prepared by a modification of our previous technique (14). Briefly, fresh citrated plasma was diluted 1:1 with 20.0 mM Tris–HCl, 10.0 mM sodium citrate, pH 7.2 (TCB), containing 0.3 M NaCl, before loading onto a heparin-agarose column. After loading, the column was washed with 5–20 vol of TCB, which contained 0.225 M NaCl, and then eluted with a 120–150-ml linear gradient from 0.225 M to 2.0 or 3.0 M NaCl. The fractions containing AT activity that eluted between ~0.5 and 0.8 M NaCl were pooled, slowly diluted to 0.3 M NaCl with the TCB buffer, and then loaded on a heparin-agarose column. After washing with 5–10 vol of TCB, which contained 0.3 M NaCl, the column was eluted with 2.0 or 3.0 M NaCl. This method of preparation produced AT that was highly concentrated (1.5–4.0 mg/ml), homogeneous on SDS-polyacrylamide gel electrophoresis, and had a heparin-cofactor activity of ~4.0 U/mg. Rabbits fibrinogen of >90% clottability was prepared by repeated precipitation of heparinized plasma with ammonium sulfate (15).

Assays. AT inhibitory activity, assayed as heparin cofactor (16), and AT antigen, assayed by rocket electroimmunoassay (17), were as reported previously (14). Fibrinogen clottability was determined by the methods described (15).

Preparations of radioiodinated proteins. AT was labeled by either the Enzymobead technique or the iodine monochloride method (18). The labeling procedure recommended by the Enzymobead manufacturer was modified in two ways: (*a*) a lower Enzymobead to protein ratio was used; (*b*) the reaction was carried out at 4°C for 2 h. For labeling, 250 μl of AT, obtained from the final purification step, was added to a mixture of 500 μl of 0.2 M phosphate buffer (pH 7.2), an aliquot of 1.3×10^{-3} M cold sodium iodide to give an iodine to protein ratio of 0.5, one-fifth vial of Enzymobead, and a trace of iodine-131 (20–200 μCi). The incorporation reaction was initiated by the addition of 250 μl of 2% alpha-D-glucose, which had been allowed to mutorotate overnight at room temperature. Iodine incorporation into AT ranged from 40 to 80%. After Enzymobead removal the reaction mixture was diluted with TCB, and loaded onto a 5.0-ml heparin-agarose column equilibrated with TCB containing 0.3 M NaCl. After washing to remove unbound iodine, the labeled protein was eluted with a linear NaCl gradient. The heparin-cofactor activity of the fractions eluting near the center of the peak of eluted radioactivity, measured as previously described (16), was essentially identical to that of the starting material. These fractions were pooled for injections.

Iodination of rabbit fibrinogen was also labeled by the Enzymobead technique. The labeled protein was freed from unincorporated iodine (15) and the clottability of the resulting [^{125}I]fibrinogen was 94–96%. Labeling of AT by the iodine monochloride method was carried out as described previously (15), with all reactants at 4°C. The labeling efficiency was 20%. Biologically screened ^{131}I-AT was prepared by injecting 100–150 μCi of ^{131}I-AT into 2.0–2.5-kg rabbits. Approximately 16 h later citrated blood was obtained from these animals by cardiac puncture, under anesthesia. Aliquots of the resulting plasma were injected into recipient animals as described below.

Animals and injections. Only healthy New Zealand white rabbits, observed for 1–3 wk, were used. The animals were placed on drinking water containing 200 mg/L potassium iodide and 1.8 g/L NaCl beginning 3 d before the injection of labeled protein (13). Labeled-protein solutions (2–10 μCi), drawn into plastic syringes, were weighed for accurate volume determination. Injections used the right lateral ear vein without tissue infiltration.

Blood sampling and handling. Blood samples were collected 5–10 min after the injections, at 2.5–3.5 h, 5–6 times over the next 48 h, and daily thereafter up to 10 d. After a razornick in the left lateral ear vein, blood was collected 9:1 in 0.129 M sodium citrate. Volume of blood was determined by weight, and by assuming that the whole blood density was 1.06 mg/ml. Duplicate microhematocrits of the whole blood and anticoagulated blood were obtained.

After centrifugation for 10 min at 2,000 × *g*, 1 ml of plasma was aspirated for counting of radioactivity. In preliminary experiments, 1 ml of whole citrated blood was also counted to determine if any of the ^{131}I-AT became associated with the formed elements. It was found that the whole blood radioactivity was identical to the radioactivity of the plasma in the sample, within limits of experimental error. Therefore, only plasma was counted for results reported below. Plasma non-protein-bound radioactivity was determined as described previously (19), except that 50 μl of 2% dexoycholate per milliliter of plasma was added before TCA precipitation.

Counting was in a Packard model 5230 (Packard Instrument Co., Downers Grove, IL) or Searle model 1197 (Searle Analytic, Inc., Des Plaines, IL) dual channel crystal scintillation counters. Counting rates of samples containing both iodine-125 and iodine-131 were corrected for iodine-131 counts which spilled into the iodine-125 channel.

Whole-body radioactivity. Whole body radioactivity (20) was determined immediately after each blood sampling. Counting was for from 2 to 25 min.

Radioactivity data corrections and analysis. All radioactivity data was first corrected for radioactive decay and background. Correction for plasma dilution by anticoagulant (F_1) was by the following formula:

$$F_1 = \frac{V_B(1 - HCT_B) + V_C}{V_B(1 - HCT_B)}, \quad (1)$$

where V_B is the volume of blood collected, V_C is the volume of anticoagulant, and HCT_B is the hematocrit/100 of the whole blood. Correction for dilution of plasma within the animal (F_2) was made by application of the following formula:

$$F_2 = (1 - HCT_B^i)/(1 - HCT_B^1), \quad (2)$$

where HCT_B^i is the whole blood hematocrit/100 of sample i, and HCT_B^1 is the whole blood hematocrit of the first sample. The radioactivity removed in each blood sample was determined by multiplying the radioactivity of the 1-ml plasma sample by $(1 - HCT_C)V_T$, where HCT_C is the hematocrit/100 of the anticoagulated blood sample and V_T is the total volume of the sample. A correction factor for removal of radioactivity in blood samples (F_3) was obtained from

$$F_3 = \frac{R}{R - \sum_{i=1}^{n-1} r_i}, \quad (3)$$

where R is the total radioactivity injected and r_i is the radioactivity removed in sample i that was corrected for decay.

To obtain protein-bound radioactivity in plasma samples, the non-TCA-precipitable radioactivity was subtracted from the radioactivity of the plasma sample. The whole body non-protein-bound radioactivity was estimated by multiplying the plasma value by a factor of 8.0 (21). Apparent plasma volumes were calculated from dilution of the ^{131}I-AT or [^{125}I]fibrinogen between injection and the first blood sample (22).

Whole body radioactivity measurements of ^{131}I-AT were also corrected for radioactivity removed by blood sampling and a decay factor, as determined by counting a plastic rabbit phantom containing water and approximately the same amount of iodine-131 injected into the animals. No deadtime correction was required for the levels of ^{131}I-AT used in these studies. Corrected whole body (C_{wb}) radioactivity was fitted to exponential equations of the form $y(t) = C_{wb}e^{-a_{wb}t}$, for $t > 1$ d. Corrected plasma protein-radioactivity was fitted to equations of the form $y(t) = C_1e^{-a_1t} + \cdots + C_ne^{-a_nt}$, where n was either 2 or 3. This analysis was performed by curve "peeling" using the NIH PROPHET computing system (23) or a programmable calculator.

Results

The in vivo behavior of ^{131}I-AT. Enzymobead protein iodination was used for label rabbit fibrinogen, a protein thats in vivo kinetic behavior has been well characterized (25), as well as to iodinate AT. Fig. 1 shows the best fit of the simultaneous disappearance of glucose oxidase-lactoperoxidase labeled ^{131}I-AT and [^{125}I]fibrinogen for a typical rabbit. The best fit of the plasma [^{125}I]fibrinogen data was obtained by a two-exponential equation, while the plasma ^{131}I-AT data was best fit by three exponentials, and give an equation of the form

$$*A_p(t) = C_1e^{-a_1t} + C_2e^{-a_2t} + C_3e^{-a_3t}. \quad (4)$$

Also shown in Fig. 1 are the iodine-131 whole body ($*A_{wb}$) and the estimated total body non-protein-bound ($*A_z$) radioactivities fitted to single exponential equations for $t > 1.0$ d. Three "young rabbits" (13, 25) gave fractional catabolic rates for [^{125}I]fibrinogen of 0.479±0.031 day^{-1}, which are not significantly different from the results obtained previously (25).

The apparent plasma volumes of six rabbits were determined from isotope dilution after simultaneous injection of [^{125}I]-fibrinogen and ^{131}I-AT. Three of these rabbits are among those

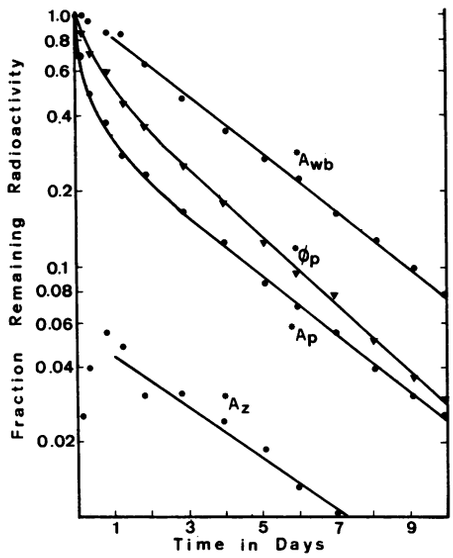

Figure 1. A semilogrithmic plot of the disappearance of radioiodine from a typical rabbit (R21) simultaneously injected with unscreened ^{131}I-AT and ^{125}I-fibrinogen. Each protein was labeled by the glucose oxidase-lactoperoxidase technique. The disappearance of whole body ^{131}I-AT, plasma ^{125}I-fibrinogen ($*Ø_p$), plasma ^{131}I-AT, and plasma non-protein-bound ^{131}I multiplied by 8.0 (16) are shown. $*A_{wb}$ and $*A_z$ data are fit to single exponential disappearance curves for $t > 1.0$ d. $*A_p$ and $*Ø_p$ data are best fit to three- and two-exponential disappearance curves, respectively.

listed in Table I and three are not, the latter because they were smaller (<2.0 kg) than the 12 animals listed. The apparent plasma volumes for the six rabbits averaged 30.6±4.1 ml/kg for [^{125}I]fibrinogen and 37.6±3.9 ml/kg for ^{131}I-AT. Statistical comparison of these data, using the paired t test, showed that this difference was significant at the $P < 0.005$ level. The plasma volumes calculated from [^{125}I]fibrinogen were equivalent to previous determinations of rabbit plasma volume using ^{131}I-labeled albumin (11). The higher apparent plasma volumes obtained from ^{131}I-AT indicated that some injected protein was transferred from the circulation to a nonplasma vascular compartment during the time interval between its injection and the blood sample obtained 5–10 min later. The decreases in plasma ^{131}I-AT between injection and the first sample were reflected in decreases in the plasma radioactivities between the first and the subsequent plasma samples, as illustrated by the results shown in Fig. 1.

Early rapid removal of ^{131}I-AT was not accompanied by a concomitant rise in radioactive breakdown products, as illustrated by the lower curve ($*A_z$) in Fig. 1. Nor was the presence of a large initial increase in $*A_z$-radioactivity, caused by early more rapid ^{131}I-AT catabolism, reflected in early more rapid whole body ^{131}I disappearance data. Thus, whole body radioactivity was fitted to a single exponential disappearance of the form $C_{wb}e^{-a_{wb}t}$, in which C_{wb} was >1.00. A test for the absence of denatured ^{131}I-AT was performed by study of the behavior of biologically screened material. The initial drop in plasma

Table I. Constants Describing Exponential Curves Fit To Rabbit Plasma and Whole-Body ^{131}I-AT

Rab. #	Wt.	I-AT* prep.	Plasma volume	Plasma parameters						Whole-body parameters		$t_{1/2}$ d	
				C_1	a_1	C_2	a_2	C_3	a_3	C_{wb}	a_{wb}	a_1	a_{wb}
	kg		*ml/kg*										
R18‡	2.51	U-1	32.5	0.344	0.278	0.365	1.974	0.305	13.36	1.14	0.266	2.49	2.61
R19‡	2.46	U-1	33.8	0.348	0.292	0.252	1.360	0.417	10.84	1.12	0.281	2.37	2.47
R21‡	2.50	U-2	34.8	0.343	0.265	0.289	1.627	0.390	10.32	1.05	0.263	2.61	2.63
B1	2.20	U-3	30.5	0.358	0.291	0.288	1.606	0.376	13.52	1.01	0.300	2.38	2.31
B2	2.42	U-3	33.0	0.308	0.307	0.480	2.249	0.224	10.50	1.05	0.306	2.25	2.26
B3	2.43	U-3	29.2	0.327	0.252	0.338	1.919	0.359	10.52	1.09	0.266	2.75	2.61
Mean	2.42		32.3	0.338	0.281	0.326	1.790	0.353	11.09	1.08	0.280	2.48	2.48
±	0.10		1.9	0.016	0.018	0.057	0.291	0.050	1.91	0.04	0.017	0.16	0.15
R17	2.49	S-1	26.4	0.380	0.279	0.395	3.273	0.248	21.66	1.22	0.290	2.48	2.39
R24	2.72	S-2	27.6	0.354	0.239	0.391	2.486	0.290	22.39	1.05	0.231	2.90	3.00
R25	2.71	S-2	31.2	0.343	0.233	0.239	1.757	0.434	9.21	1.07	0.241	2.92	2.88
B4	2.65	S-3	30.6	0.323	0.286	0.228	1.479	0.452	9.93	1.15	0.288	2.41	2.41
B5	2.68	S-3	33.0	0.347	0.259	0.288	2.210	0.390	14.32	1.34	0.257	2.70	2.69
B6	3.00	S-3	32.7	0.324	0.235	0.297	1.891	0.404	13.69	1.38	0.264	2.92	2.63
Mean	2.71		30.2	0.345	0.255	0.306	2.183	0.370	15.70	1.20	0.262	2.72	2.67
±SD	0.15		2.5	0.019	0.021	0.066	0.584	0.075	5.17	0.13	0.022	0.21	0.22

* [^{131}I]AT preparations labeled with "S" were biologically screened, and those labeled with "U" were unscreened. The S-3 [^{131}I]AT was labeled by the iodine monochloride method; all other preparations were labeled by the Enzymobead technique. ‡ Simultaneously injected with [^{131}I]AT and [^{125}I]fibrinogen.

^{131}I-AT was also observed under these conditions, as illustrated in Fig. 2.

Table I summarizes the values of the constants from Eq. 4 that best fit the plasma radioactivity data for six young rabbits injected with unscreened ^{131}I-AT and six each injected with screened ^{131}I-AT. The screened material was prepared by either the glucose oxidase-lactoperoxidase or iodine monochloride methods. Also shown in Table I are the constants that describe the best fit of whole body data to single exponential equations.

Calculation of catabolic rate and AT-compartment masses. The methods used for determination of fractional catabolic rates (j_3, $j_{3.5}$, and j_T) are summarized in the Appendix. The values of the C's and a's, given in Table I, were first used to obtain j_3 for each animal. These are given in Table II, and average 0.673±0.051 and 0.716±0.048 day^{-1} for screened and unscreened ^{131}I-AT, respectively. We can obtain the absolute rate of rabbit AT catabolism, absolute antithrombin III catabolic rate (ACR) because

$$ACR = j_3 \bar{A}_p, \quad (5)$$

where $\bar{A}_p$ is the total plasma AT mass, as obtained from the product of plasma volume and plasma AT concentration. The average plasma-AT concentration during the course of AT turnover studies for six rabbits was 254±24 μg/ml, as obtained by rocket immunoelectrophoresis, and the plasma volume for the

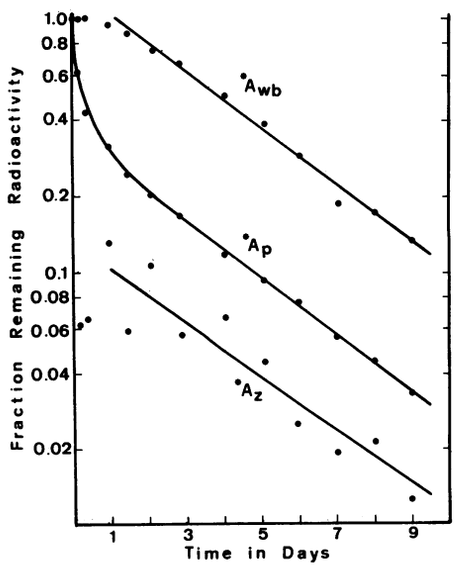

Figure 2. A semilogrithmic plot of the disappearance of ^{131}I from a typical rabbit (BS) injected with screened ^{131}I-AT labeled by the iodine monochloride technique. The disappearance of whole body, plasma, and non-protein-bound radioactivities are shown. *A_{wb} and *A_z data are fit to single exponential disappearance curves for $t > 1.0$ d. *A_p data are fit to a three-exponential disappearance curve.

Table II. Daily Fractional Catabolic Rate Constants for AT from the Analysis of Radioiodinated-AT (I-AT) Disappearance Obtained for the Rabbits Listed in Table I

Constant	Unscreened I-AT	Screened I-AT	All I-AT
j_3	0.716±0.048	0.673±0.052	0.695±0.054
$j_{3\cdot5}$	0.487±0.075	0.434±0.049	0.461±0.069
j_T	0.224±0.013	0.225±0.016	0.235±0.018
j_{3D}*	0.721±0.047	0.680±0.056	0.707±0.056
j_T/A_p‡	0.716±0.070	0.685±0.095	0.700±0.085

* Determined from computer-derived solution of differential equations.
‡ A_p was determined from mass balance data.

rabbits injected with [^{125}I]fibrinogen was ~80 ml. Substituting the product of these values into Eq. 5 gives an approximate absolute AT-catabolic rate of 14 mg/d or 5.6 mg/kg per d.

$j_{3\cdot5}$, the rate of AT catabolism as a fraction of the AT in compartments A_p and A_w (the compartment with which plasma ^{131}I-AT very rapidly equilibrates), for screened and unscreened ^{131}I-AT, averaged 0.434±0.049 and 0.487±0.075 day^{-1}, respectively (Table II). The absolute catabolic rate is related to $j_{3\cdot5}$ in a similar way that j_3 is, as given in Eq. 5. Thus,

$$ACR = j_{3\cdot5}(\bar{A}_p + \bar{A}_w). \quad (6)$$

Since the AT mass in the $\bar{A}_w$ compartment is unknown, the absolute rate cannot be obtained from Eq. 6. However, because the absolute catabolic rate is a constant,

$$j_3\bar{A}_p = j_{3\cdot5}(\bar{A}_p + \bar{A}_w). \quad (7)$$

Substituting j_3, $j_{3\cdot5}$, and the value of $\bar{A}_p$ into Eq. 7, the mass of AT in compartment A_w ($\bar{A}_w$) can be calculated. Thus, a value of 11.7 mg or 4.7 mg/kg was obtained.

j_T, the fractional rates of AT breakdown from the total body AT pool, were 0.225±0.016 and 0.244±0.013 day^{-1} for screened and unscreened ^{131}I-AT, respectively (Table II). The total body AT pool is distributed among three physiological compartments, A_p, A_w, and A_e; thus, the absolute catabolic rate is related to j_T as follows:

$$ACR = j_T(\bar{A}_p + \bar{A}_w + \bar{A}_e). \quad (8)$$

This equation can be combined with Eq. 5 to give

$$j_3\bar{A}_p = j_T(\bar{A}_p + \bar{A}_w + \bar{A}_e). \quad (9)$$

Substituting the previously calculated values of j_3, $\bar{A}_p$, $\bar{A}_w$, and j_T, the mass of AT outside the vascular system, $\bar{A}_e$, is 32.2 mg or 12.9 mg/kg.

Calculation of the relative sizes of the plasma, noncirculating vascular and extravascular compartments. The fraction of total body AT in each of the three physiological compartments has been calculated from (1) the ^{131}I-AT disappearance data and a mass-balance relationship, or (2) the rates of breakdown given in the previous section. Using the first method, a fraction of 0.337±0.031 was calculated for AT in plasma, A_p, from the relationship

$$A_p = {}^*A_p(t)/[{}^*A_{wb}(t) - {}^*A_z(t)], \quad (10)$$

where *A is the labeled-AT in the respective compartment, and $t > 2.5$ d after ^{131}I-AT injection (19). During this time the ^{131}I-AT is in a steady state with respect to distribution between compartments. For each animal an average of A_p was obtained from plasma, whole body, and $^*A_z$-compartment radioactivity data up to $t = 10$ d. Because a significant fraction of the ^{131}I-AT was transferred from the circulation to the vascular-associated compartment before the first blood sample was taken, $^*A_p(t)$ and $^*A_z(t)$ were corrected to account for this by dividing each fraction by $C_1 + C_2 + C_3$.

As discussed in the Appendix, at the time the first "steady state" has been achieved ($t = SS_1$), the plasma and vascular-associated compartments can be considered as a single compartment. Only distribution of ^{131}I-AT to the extravascular space, giving rise to C_2 and a_2, and catabolism of ^{131}I-AT, giving rise to C_1 and a_1, are then detected. For a two compartment system, when using an undenatured labeled-protein, $C_1 + C_2$ is equal to the fraction of radioactivity of the labeled-protein present in the plasma at $t = 0$ (12). Thus, for ^{131}I-AT, after equilibrium between plasma and vascular-asssociated compartments has been achieved,

$$C_1 + C_2 = {}^*A_p(SS_1). \quad (11)$$

$^*A_p(SS_1)$ is equal to the fraction of the total vascular-^{131}I-AT still free in the plasma alone. This fraction is constant after $t = SS_1$, and at any given time is equal to plasma ^{131}I-AT, $^*A_p$, divided by the sum of $^*A_p$ and the ^{131}I-AT in the vascular-associated compartment, $^*A_w$. Since

$${}^*A_p(t)/[{}^*A_p(t) + {}^*A_w(t)] = A_p/(A_p + A_w), \quad (12)$$

then,

$$C_1 + C_2 = A_p/(A_p + A_w). \quad (13)$$

A_p, as calculated by Eq. 10, and $C_1 + C_2$ were substituted into Eq. 13, and gave 0.178±0.056 for the average fraction of AT in the vascular-associated compartments, A_w (Table III). Since the sum of the fractions A_p, A_w, and A_e must equal 1.00, an average A_e fraction of 0.485±0.069 was obtained.

The method described in the previous section for calculation of $\bar{A}_p$, $\bar{A}_w$, and $\bar{A}_e$ was also used to calculate A_p, A_w, and A_e. Combining Eqs. 5, 6, and 8, and expressing $\bar{A}_p$, $\bar{A}_w$, and $\bar{A}_e$ as fractions of the total body AT, A_p, A_w, and A_e,

$$j_3A_p = j_{3\cdot5}(A_p + A_w) = j_T(A_p + A_w + A_e). \quad (14)$$

Since $A_p + A_w + A_e = 1.00$,

$$j_3A_p = j_{3\cdot5}(A_p + A_w) = j_T. \quad (15)$$

Thus,

$$A_p = j_T/j_3, \quad (16)$$

Table III. Sizes of the Plasma (A_p), Vascular-associated (A_w), and Extravascular (A_e) AT Compartments, Calculated from Radioiodinated AT (I-AT) Disappearance Data, for the Rabbits Listed in Table I

Compartment	Calculation* method	Unscreened I-AT (SD)	Screened I-AT (SD)	All I-AT (SD)
A_p	M.B.	0.343±0.028	0.332±0.033	0.337±0.031
	K.C.	0.341±0.013	0.335±0.012	0.338±0.013
A_w	M.B.	0.171±0.048	0.185±0.062	0.178±0.056
	K.C.	0.173±0.045	0.188±0.053	0.180±0.050
A_e	M.B.	0.486±0.067	0.484±0.072	0.485±0.069
	K.C.	0.486±0.057	0.478±0.045	0.482±0.051

* Values labeled M.B. were determined by the mass-balance approach; those labeled K.C. were derived from the kinetic constants, as determined by curve-peeling methods.

and

$$A_w = j_T/j_{3\cdot 5} - A_p. \quad (17)$$

Finally,

$$A_e = 1.00 - A_p - A_w. \quad (18)$$

The results obtained for the compartment sizes determined by this approach are essentially identical with those obtained using the mass-balance method (Table III).

Discussion

The study of the in vivo kinetic behavior of radiolabeled AT results in a third generation of in vivo kinetic analyses of plasma proteins. The first generation studies were those conducted on albumin (e.g. references 11 and 24), a molecule thats in vivo distribution seems to be determined solely by hydrodynamic and concentration-dependent properties. Later plasma proteins studied were capable of undergoing activation from zymogen forms (e.g. references 25, 26, and 27). In the in vivo study of AT we are dealing with a molecule which, in addition to its hydrodynamic and concentration-dependent properties, and its ability to be converted from one form to another, also interacts with vascular endothelial cells (9).

Here we show that the interaction of plasma AT with another vascular site is detectable by analysis of data describing the in vivo kinetic behavior of rabbit ^{131}I-AT. Thus, a nonplasma vascular-AT pool or compartment is demonstrated by rapid initial decreases in plasma ^{131}I-AT, which is reflected in the high apparent ^{131}I-AT plasma volume and the requirement of a fast third exponential to describe plasma ^{131}I-AT disappearance. In addition to our data, the early rapid disappearance of radioiodinated-AT has also been reported by others in studies of the disappearance of ^{131}I-AT from rabbit plasma during the first 5 h after injection (28). Our data were not the result of denaturation of AT during purification or iodination, which is demonstrated by the identical results with screened and unscreened ^{131}I-AT, which are labeled by either the immobilized lactoperoxidase-glucose oxidase or by iodine monochloride methods. Furthermore, rapid removal of altered ^{131}I-AT by catabolism is ruled out because of the absence of high levels of non-protein-bound iodine during the period corresponding to rapid ^{131}I-AT removal, and correspondingly, to C_{wb} values of >1.00. A final proof of the suitability of our ^{131}I-AT preparations to trace in vivo AT behavior comes from the j_T/A_p data, which, shown by Eq. 15 (see also the Appendix), is equal to j_3. Because j_T and A_p, as obtained from by mass-balance, are dependent on data obtained in the steady state, any denatured material has been removed. Therefore, j_3 calculated from j_T/A_p is independent of the presence of any denatured ^{131}I-AT injected. As shown in Table II, agreement between the values of j_T/A_p and j_3 calculated by curve peeling or direct computer fitting was obtained. Based on these data, and since no ^{131}I-AT is detectable in association with circulating blood cells, we conclude that the initial rapid decrease in plasma ^{131}I-AT is the result of a pool of vascular-endothelial AT binding sites.

Because the size of the nonplasma vascular-associated compartment (A_w) is a significant fraction of the total vascular-AT, plasma AT levels alone may not reflect the true vascular AT level of an individual. Thus, the size of the A_w pool may vary in health and disease, genetically, or with age. This could explain discrepancies between measured AT plasma levels and clinical states.

Several types of compartmental kinetic models might describe the plasma and whole body radioactivities obtained after injection of ^{131}I-AT in the rabbit. The simplest one would be the three-compartment model, which was proposed by Matthews (10). As shown in Fig. 3 *A*, this consists of a central plasma compartment into which ^{131}I-AT is injected, and of two other compartments that exchange with the plasma independently. Calculation of j_3 was originally derived from this type of model (10). Another reasonable compartmental model, among those possible, is shown in Fig. 3 *B*. In this series, or continuous model, AT is seen as moving from the plasma through the rapidly-equilibrating compartment to the extravascular space. This model considers that a pool of AT binding sites mediates the transfer of AT from plasma to interstitial fluids in a manner consistent with receptor-mediated formation of vesicles (29). These could move across the endothelium as postulated by Renkin (30).

Breakdown of AT in the models shown in Fig. 3 could be from any of the compartments. It has been suggested previously that AT breakdown occurs from the extravascular compartment, because a delay in the disappearance of total body radioactivity was observed in the dog and the human (31). We have also observed this in the majority of our studies. To test this hypothesis for the rabbit, the system of differential equations describing each model was fitted to the plasma ^{131}I-AT disappearance data for each animal, using an iterative curve-fitting

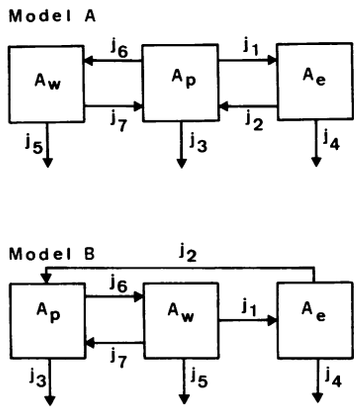

Figure 3. Two models for the three compartment distribution and catabolism of AT in the rabbit. Model A, the independent compartments model, represents AT as being transferred to and from a central plasma compartment, A_p, to and from two unrelated compartments, A_w and A_e. Model B, the series or continuous transport model, represents AT as being transferred from a central plasma compartment, A_p, to the extravascular compartment, A_e, via a mediating compartment, A_w. In both models, newly synthesized AT is released into the plasma compartment and catabolism can occur in association with any compartment.

algorithm. The fitting was performed using the PROPHET computing system (23), and using the public procedure "DIFFEQ". For each model, two variations were fitted: $j_4 = j_5 = 0$ and $j_3 = j_5 = 0$. The values of j_3 obtained from either model were essentially identical to those obtained using Eq. 5 (see Table II).

Next, the solutions of the differential equations for each model were computer integrated, and the predicted values of the fractions of $*A_p$, $*A_w$, and $*A_e$ were obtained at the time of each blood sampling. At each of these times the sum of the predicted $*A_p(t)$, $*A_w(t)$, and $*A_e(t)$ was added to the estimated total non-protein-bound radioactivities, which were determined from the non-TCA-precipitable radioactivity. This gave predicted whole body radioactivities for each catabolic-site variation of models A or B. If breakdown was from the same compartment, the predictions of whole body radioactivity were essentially identical for the two models. Fig. 4 shows the ^{131}I-AT whole body and plasma data and predictions for a typical rabbit. In this case, the whole body data rests about halfway between breakdown modeled from plasma and breakdown modeled from the extravascular compartment. Comparison of predictions with data for other animals gave variable results. In some cases the

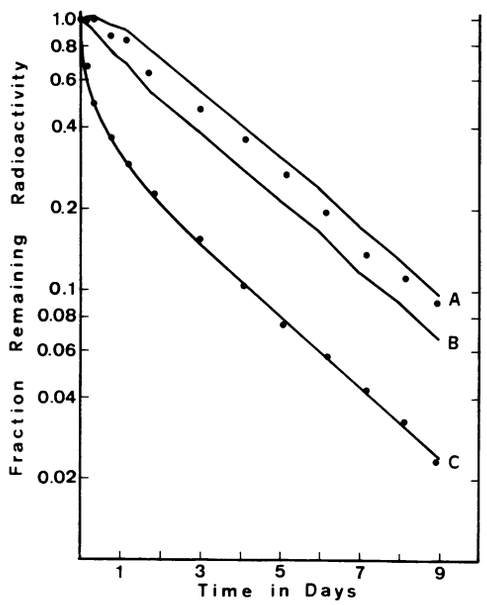

Figure 4. Comparison of ^{131}I-AT disappearance data with predicted disappearance of plasma and whole body radioactivities for a typical rabbit, R19. Curve A shows the sum of the predicted plasma, $*A_p$, noncirculating vascular, $*A_w$, and extravascular, $*A_e$, radioactivities added to the estimated non-protein-bound radioactivity, when catabolism is assigned exclusively to compartment A_e. Curve B gives the same sum when breakdown is assigned exclusively to compartment A_p. Curve C is the predicted plasma AT radioactivity, $*A_p$, if breakdown is assigned to either A_p or A_e. The data points (•) are actual measured whole body (*top*) and plasma (*bottom*) radioactivities.

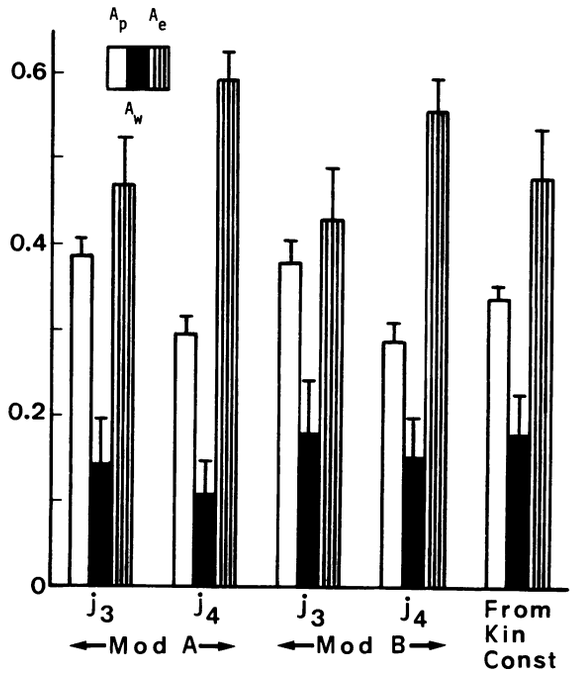

Figure 5. Comparison of fractional compartment sizes derived from computer modeling of plasma ^{131}I-AT radioactivity, and from the kinetic constants method. Each catabolic site variation of models A and B was fit to the set of differential equations describing it. The solutions to these equations were integrated and the fractional compartment sizes were determined in the steady state. The groups of compartment sizes labeled j_3 were obtained by assuming that catabolism occurs from the plasma compartment alone, while those labeled j_4 were the result of assuming that catabolism occurs from the extravascular compartment only. The data on the right was calculated from the kinetic constants, j_3, $j_{3\cdot5}$, and j_T. Error bars represent 1SD. Kin Const, kinetic constant; Mod A, Mod B, models A and B.

data was more closely predicted by breakdown from plasma (e.g. rabbit R21, shown in Fig. 1), while others were closer to the prediction when breakdown was from the extravascular compartment (e.g. rabbit B5, shown in Fig. 2). Generally, the data rested somewhere between the predictions obtained for breakdown from plasma and breakdown from extravascular space. These findings suggest that breakdown is not confined to a single compartment in rabbit, but that it occurs to variable degrees in both vascular and extravascular areas.

Mean sizes of the three compartments predicted by each kinetic model and those calculated directly from the radioactivity data are shown in Fig. 5. The average differences for A_w were 0.056 ± 0.030 for model A and 0.013 ± 0.032 for model B, which, using a paired t test, were significantly different at the $P < 0.0001$ level. This suggests that model B, passage of AT from plasma to extravascular space via compartment A_w, best describes the in vivo behavior of rabbit AT.

In vivo kinetic analysis of radioiodinated AT in man (32, 33, 34) and dog (19, 35, 36) has been done previously by several investigators, but none have reported the presence of additional physiological AT compartments. The reason for the difference between our data and those of others may be partly species related. Preliminary studies on the behavior of human ^{131}I-AT indicate that a significantly smaller A_w pool is present in man.

Appendix

It has been shown previously by Reeve and Bailey (12) that the fractional catabolic rate, j_3, for a radioiodinated protein, *P, is related to its plasma disappearance, $*P_p dt$, in the following manner: $j_3 \int_0^\infty *P_p dt = R$, where j_3 and R are constants. As shown (12), when $*P_p dt$ is described by a sum of exponentials,

$$j_3 \int_0^\infty \sum_{i=1}^{n} C_i e^{-a_i t} dt = R, \tag{A1}$$

where R is the total plasma radioactivity at $t = 0$. j_3 can be obtained from the integrated form of Eq. A1:

$$j_3 = \sum_{i=1}^{n} C_i / \sum_{i=1}^{n} C_i/a_i, \tag{A2}$$

where $\sum_{i=1}^{n} C_i = R$ and the a's are constants. As shown above, rabbit ^{131}I-AT disappearance is best described by three-exponential equations. Thus,

$$j_3 = (C_1 + C_2 + C_3)/(C_1/a_1 + C_2/a_2 + C_3/a_3). \tag{A3}$$

If the first plasma sample after ^{131}I-AT injection was obtained after equilibrium between A_p and A_w had been achieved, the data obtained would be consistent with a two compartment system. Therefore, the disappearance of labeled-AT would be described by a two-exponential disappearance curve of the following form:

$$*A_p(t) = C_1' e^{-a_1 t} + C_2' e^{-a_2 t}, \tag{A4}$$

where C_1' and C_2' are a different set of constants than those obtained from the three-exponential curve. Under these conditions the fractional breakdown rate, $j_{3 \cdot 5}$, can be calculated from the following form of Eq. A2:

$$j_{3 \cdot 5} = (C_1' + C_2')/(C_1'/a_1 + C_2'/a_2), \tag{A5}$$

where the fractions $C_1'/(C_1' + C_2')$ and $C_2'/(C_1' + C_2')$ are equal to $C_1/(C_1 + C_2)$ and $C_2/(C_1 + C_2)$, which were obtained from the complete three-exponential $*A_p(t)$ data. Since a_1 and a_2 are not effected by shifting the time of initial sampling, Eq. A5 becomes

$$j_{3 \cdot 5} = (C_1 + C_2)/(C_1/a_1 + C_2/a_2). \tag{A6}$$

The fractional catabolism of any plasma protein, P, can also be determined from the steady state portion of the *P-plasma or *P-whole body disappearance curves. Thus, after a steady state has been achieved with regard to distribution, the fraction of remaining labeled protein, F, at some later time, t, is described by

$$F = e^{-at}, \tag{A7}$$

in which "a" is a constant. For a constant time period during the steady state, the fraction of the remaining labeled protein that disappears is a constant, j, and is equal to

$$j = \frac{F_1 - F_2}{F_1} = \frac{e^{-a(t_1)} - e^{-a(t_2)}}{e^{-a(t_1)}}, \tag{A8}$$

where F_1 is the fraction of labeled protein at t_1 and F_2 is the fraction at t_2. For any 24-h period the fractional catabolic rate, calculated from Eq. A8, is the constant we have called j_T. For example, the calculation of j_T can be determined between $t = 0$ and $t = 1$ d, in which case

$$j_T = 1 - e^{-a}. \tag{A9}$$

Hence, for a protein distributing to n compartments, each containing a fraction, P_i, of the total P, such that

$$P_1 + P_2 + P_3 + \cdots + P_n = 1.0, \tag{A10}$$

we can say that

$$j_T = j_T(P_1 + P_2 + P_3 + \cdots + P_n). \tag{A11}$$

This allows determination of the catabolic rate as a fraction of the P in any physiological compartment, P_i. For example, once we obtain the fraction of P in the plasma, P_p, from the steady state plasma and whole body disappearance of the radiolabeled protein, *P (see Results), then the fraction of P catabolized per day, expressed as a fraction of P_p, can be calculated. This fractional catabolic rate, j_3, is thus obtained from

$$j_T = j_3 P_p. \tag{A12}$$

For any compartment

$$j_T = j_i P_i, \tag{A13}$$

where P_i is the fraction of total P in compartment i, and j_i is the fractional rate of catabolism of P_i. Furthermore, if the sizes are known for two compartments, P_i and $P_{(i+1)}$,

$$j_T = j_{i \cdot (i+1)}[P_i + P_{(i+1)}], \tag{A14}$$

where $j_{i \cdot (i+1)}$ is the fraction of the sum of P in compartments $P_i + P_{(i+1)}$ catabolized each day. Thus, for AT,

$$j_T = j_3 A_p = j_{3 \cdot 5}(A_p + A_w) = j_T(A_p + A_w + A_e). \tag{A15}$$

Acknowledgments

This work was supported in part by the National Institutes of Health grant 2S07-RR05583 and by a grant from Blood Systems Research Foundation, Scottsdale, AZ.

References

1. Abildgaard, U. 1969. Binding of thrombin to antithrombin. *Scand. J. Clin. Lab. Invest.* 24:23–37.

2. Yin, E. T., S. Wessler, and P. J. Stoll. 1971. Biological properties of the naturally occurring plasma inhibitor to activated Factor X. *J. Biol. Chem.* 246:3703–3711.

3. Rosenberg, J. S., P. W. McKenna, and R. D. Rosenberg. 1975. Inhibition of human factor IXa by human antithrombin-heparin cofactor. *J. Biol. Chem.* 250:8883–8888.

4. Egeberg, O. 1965. Inherited antithrombin deficiency causing thrombophilia. *Thromb. Diath. Haemorrh.* 13:516–530.

5. Collen, D., F. DeCock, and M. Verstraete. 1977. Quantitation of thrombin-antithrombin III complexes in human blood. *Eur. J. Clin. Invest.* 7:407–411.

6. Rosenberg, R. D. 1977. Chemistry of the hemostatic mechanism and its relationship to the action of heparin. *Fed. Proc.* 36:11–18.

7. Lollar, P., and W. G. Owen. 1980. Clearance of thrombin from circulation in rabbits by high-affinity binding sites on endothelium. *J. Clin. Invest.* 66:1222–1230.

8. Jacobsson, K.-G., and U. Lindahl. 1979. Attempted determination of endogenous heparin in blood. *Thromb. Haemostasis.* 42:84.

9. Busch, C., and W. G. Owen. 1982. Identification in vitro of an endothelial cell surface cofactor for antithrombin III. *J. Clin. Invest.* 69:726–729.

10. Matthews, C. M. E. 1957. Theory of tracer experiments with ^{131}I labelled plasma proteins. *Phys. Med. Biol.* 2:36–53.

11. Reeve, E. B., and J. E. Roberts. 1959. The kinetics of the distribution and breakdown of I^{131}-albumin in the rabbit. *J. Gen. Physiol.* 43:415–444.

12. Reeve, E. B., and H. R. Bailey. 1962. Mathematical models describing the distribution of I^{131}-albumin in an. *J. Lab. Clin. Med.* 60:923–943.

13. Atencio, A. C., H. R. Bailey, and E. B. Reeve. 1965. Studies on the metabolism and distribution of fibrinogen in young and older rabbits. I. Methods and models. *J. Lab. Clin. Med.* 66:1–19.

14. Carlson, T. H., and A. C. Atencio. 1982. Isolation and partial characterization of two distinct types of antithrombin III from rabbit. *Thromb. Res.* 27:23–34.

15. Atencio, A. C., D. C. Burdick, and E. B. Reeve. 1965. An accurate isotope dilution method for measuring plasma fibrinogen. *J. Lab. Clin. Med.* 66:137–145.

16. Ablidgaard, U., M. Lie, and O. R. Odegard. 1977. Antithrombin (heparin cofactor) assay with "new" chromogenic substrates (S-2238 and Chromozym TH). *Thromb. Res.* 11:549–553.

17. Laurell, C.-B., and E. J. McKay. Electroimmunoassay. *Methods Enzymol.* 73:339–369, 1981.

18. McFarlane, A. S. 1959. Efficient trace-labelling of proteins with iodine. *Nature (Lond.).* 182:53.

19. Reeve, E. B., B. Leonard, S. H. Wentland, and P. Damus. 1980. Studies with ^{131}I-labelled antithrombin in dogs. *Thromb. Res.* 20:375–389.

20. Atencio, A. C., K. Joiner, and E. B. Reeve. 1969. Experimental and control systems studies of plasma fibrinogen regulation in rabbits. *Am. J. Physiol.* 216:764–772.

21. Zizza, F., T. J. Campbell, and E. B. Reeve. 1959. The nature and rates of excretion of radioactive breakdown products of I^{131}-albumin in the rabbit. *J. Gen. Physiol.* 43:397–413.

22. Reeve, E. B., and J. J. Franks. 1956. Errors in plasma volume measurement from absorption losses of albumin-I^{131}. *Proc. Soc. Exp. Biol. Med.* 93:299–302.

23. Raub, W. F. 1974. The PROPHET system and resource sharing. *Fed. Proc.* 33:2390–2392.

24. Sterling, K. 1951. The turnover of serum albumin in man as measured by I^{131} tagged albumin. *J. Clin. Invest.* 30:1228–1237.

25. Atencio, A. C., and E. B. Reeve. 1965. Studies on the metabolism and distribution of fibrinogen in young and older rabbits. II. Results. *J. Lab. Clin. Med.* 66:20–33.

26. Takeda, Y. 1970. Studies on the effects of heparin, Coumadin, and vitamin K on prothrombin metabolism and distribution in calves with the use of iodine-125-prothrombin. *J. Lab. Clin. Med.* 75:355–381.

27. Collen, D., G. Tytgat, H. Claeys, M. Verstraete, and P. Wallen. 1972. Metabolism of plasminogen in healthy subjects: effects of trans-examic acid. *J. Clin. Invest.* 51:1310–1318.

28. Koj, A., and E. Regoeczi. 1978. Effect of experimental inflammation on the synthesis and distribution of antithrombin III and α_1-antitrypsin in rabbits. *Br. J. Exp. Pathol.* 59:473–481.

29. Goldstein, J. L., R. G. W. Anderson, and M. S. Brown. 1979. Coated pits, coated vesicles, and receptor mediated endocytosis. *Nature (Lond.).* 279:679–685.

30. Renkin, E. M. 1980. Transport of proteins by diffusion, bulk flow and vesicular mechanisms. *Physiologist.* 23:57–61.

31. Reeve, E. B., B. Leonard, and T. Carlson. 1981. Kinetic studies *in vivo* of antithrombin III. *Ann. NY. Acad. Sci.* 370:680–694.

32. Collen, D., J. Schetz, F. DeCock, E. Holmer, and M. Verstraete. 1977. Metabolism of antithrombin III (heparin cofactor) in man: effects of venous thrombosis and of heparin administration. *Eur. J. Clin. Invest.* 7:27–35.

33. Chan, V., C. L. Lai, and T. K. Chan. 1981. Metabolism of antithrombin III in cirrhosis and carcinoma of the liver. *Clin. Science Mol. Med.* 60:681–688.

34. Ambruso, D. R., B. D. Leonard, R. D. Bies, L. Jacobson, W. E. Hathway, and E. B. Reeve. 1982. Antithrombin III deficiency: decreased synthesis of a biochemically normal molecule. *Blood.* 60:78–83.

35. Kobayashi, N., Y. Takeda. 1977. Effects of a large dose of oestradiol on antithrombin III metabolism in male and female dogs. *Eur. J. Clin. Invest.* 7:373–381.

36. Kobayashi, N., H. Tanaka, T. Ueno, H. Gonmori, and T. Maekawa. 1978. Studies on antithrombin III. Purification of canine and antithrombin III and its properties. *Blood & Vessel.* 9:139–144.